Polymer 51 (2010) 35–45

Contents lists available at ScienceDirect

Polymer

journal homepage: www.elsevier.com/locate/polymer

Synthesis and characterization of chiral and thermo responsive amphiphilic conetworks

Jan Tobis [a], Yi Thomann [a], Joerg C. Tiller [b,*]

[a] Freiburg Material Research Center and Institute for Macromolecular Chemistry, University of Freiburg, Stefan-Meier-Str. 21, D-79104 Freiburg, Germany
[b] Department of Bio-und Chemical Engineering, TU Dortmund, Emil-Figge-Str. 66, D-44227 Dortmund, Germany

ARTICLE INFO

Article history:
Received 15 September 2009
Received in revised form
22 October 2009
Accepted 23 October 2009
Available online 6 November 2009

Keywords:
Chiral
Hydrogel
Amphiphiles

ABSTRACT

Amphiphilic polymer conetworks (APCN) combine the properties of different polymers on the nanoscale affording advanced materials with unique properties. Here, we present the first APCN with a chiral hydrophilic phase. The conetworks were prepared by copolymerizing the tailored chiral monomer (R)-*N*-(1-hydroxybutan-2-yl)acrylamide (R-HBA) with two different crosslinkers that consist of bitelechelic methacrylate-terminated poly(dimethylsiloxane) (PDMS) of a molecular weight of 1100 g/mol and 5620 g/mol, respectively. The resulting polymer conetworks P-R-HBA-*l*-PDMS exhibited both two different T_g values, indicating nanophase separation. However, the conetwork with $PDMS_{1.1}$ did not show nanophases in the AFM and did not swell the phases separately in orthogonal solvents. On the other hand the materials with $PDMS_{5.6}$ acted like a typical APCN. The APCN P-R-HBA-*l*-$PDMS_{5.6}$ was found to be temperature sensitive in water, decreasing its degree of swelling linearly with increasing temperature. Additionally, the conetwork is increasing its degree of swelling in *n*-heptane in the region of the T_g of the P-R-HBA phase. The impact of the chiral polymer on the release of *cinchona* alkaloids was examined. For example, (−)-cinchonine diffuses four times faster off the P-R-HBA-*l*-PDMS networks than off the P-S-HBA-*l*-PDMS conetworks.

1. Introduction

An amphiphilic polymer conetwork (APCN) [1] consists of two immiscible polymers covalently bound to each other. Due to the incompatibility of the polymers a phase separation occurs. The covalent attachment prevents a macroscopic phase separation and ordered nanometer domains, resembling block copolymer structures, are observed. Thus, APCNs are optically clear materials with a huge interface. That was demonstrated on several examples with AFM, TEM, NMR, SAXS or SANS measurements [2–6]. One of the main features of APCNs is the separate swell ability of the polymer segments in hydrocarbons and in polar solvents with preservation of the structure [7,8]. These unique properties have found several applications. APCNs are excellent materials for soft contact lenses [9] because of their high oxygen and water permeability. They are suitable as scaffolds for tissue engineering [10,11], extraction of organic solvents from water [12], hosts for the growth of CdS semiconducting nanocrystals [13] and shape memory materials [14], drug release systems [15,16], carriers for aqueous ring closing metathesis catalysts [17] and for biocatalysts in non-aqueous media [18–20], biosensors [21] and chemical sensors for gaseous chlorine and vaporous acids [22]. Until now many different APCNs have been described. They mostly consist of poly(dimethylsiloxane) [3,19], poly(isobutylene) [23], PEG [24,25], poly(oxazolines) [26], poly(tetrahydrofuran) [27,28] or perfluorinated macromonomers [17,20,29–33], copolymerized with various acrylates, e.g., acrylic acid [16], NIPAM [27] or 2-(Dimethylamino) ethyl methacrylate [34]. Although, numerous variations of the polymer phases have been realized, there is no APCN known that features a chiral phase. Such an APCN would be very favourable in many applications such as separation membranes for racemates and ligating carriers for chiral, immobilized catalysts and biocatalysts.

Here, we describe the synthesis of a chiral APCN and its surprising properties, particularly with respect to the unique properties of the novel hydrophilic polymer that was designed to form the hydrophilic phase.

2. Experimental section

2.1. Materials

Silanol terminated poly(dimethysiloxane) was kindly provided by Wacker (Munich, Germany). The photoinitiator irgacure 184

* Corresponding author.
E-mail address: joerg.tiller@bci.tu-dortmund.de (J.C. Tiller).

0032-3861/$ – see front matter © 2009 Elsevier Ltd. All rights reserved.
doi:10.1016/j.polymer.2009.10.055

(1-Hydroxy-cyclohexyl-phenyl-ketone) was a gift from Ciba (Basel, Switzerland). Acryloyl chloride and chlorotrimethylsilane were purchased from Sigma–Aldrich and were used without further purification. 2-Aminobutan-1-ol and R-2-Aminobutan-1-ol (technical grade) were purchased from Fluka and were used without further purification. S-2-Aminobutan-1-ol was purchased from Molekular (Shaftesbury, UK). Ethyl acetate was washed with aqueous 5% Na_2CO_3 and saturated aqueous NaCl. It was dried with $MgSO_4$ and subsequently by refluxing over calcium hydride. It was distilled prior use. Dichloromethane was washed with conc. H_2SO_4, dest. water and aqueous 5% Na_2CO_3. It was dried with $MgSO_4$ and subsequent by refluxing over calcium hydride. It was freshly distilled prior use. The glass slides were kindly provided by Marienfeld (Lauda-Königshofen, Germany). Adhesive poly(propylene)-tape (PP; Tesafilm, Tesapack 4024) was purchased from Tesa AG (Hamburg, Germany).

2.2. Methods

NMR spectra were recorded with a Bruker ARX 300 spectrometer. Attenuated total reflection Fourier transformation infrared spectroscopy (ATR-FT-IR) was carried out on a Bruker Vektor 22 spectrometer, equipped with a Golden Gate accessory (Specac). UV–vis spectra were recorded with an Analytik Jena Specord 210 (Jena, Germany). The tapping-mode atomic force microscopy (AFM) was carried out with MultiMode AFM and nanoscope IIIa controller (Digital Instruments) at ambient conditions in phase mode and by using NCL-W (Taping Mode) cantilevers (Nanosensors, Neuchatel, Switzerland). The samples were microtomed at cryo conditions using a Leica Ultra Microtom and a Diatome diamond knife. The cut surfaces were investigated with AFM. Differential scanning calorimeter (DSC) thermographs of conetworks were recorded on a Perkin–Elmer DSC-7 from −150 to 50 °C and from −50 to 100 °C under a nitrogen atmosphere at a heating rate of 10 K/min at each of the three cycles. The weight of the samples was 10–15 mg.

2.3. Synthesis of α,ω-dimethacryloylpropylpoly(dimethylsiloxane) ($PDMS_{x,y}$)

The synthesis of $PDMS_{x,y}$ was carried out as previously reported [3]. α,ω-silanol terminated poly(dimethylsiloxane) was converted with 3-(chlorodimethylsilyl)propyl methacrylate to obtain $PDMS_{1.1}$ $M_n = 1150$ g/mol, $M_w/M_n = 1.1$ (GPC in $CHCl_3$), and $PDMS_{5.6}$ $M_n = 5620$ g/mol, $M_w/M_n = 1.8$ (GPC in $CHCl_3$, PS standards) respectively. A degree of functionalization of 99% was achieved.

2.4. Synthesis of (R)-N-(1-(trimethysilyloxy)butan-2-yl)acrylamide (R-TMSBA)

R-2-Aminobutan-1-ol (3 ml, 30.3 mmol) was added to a solution of hexamethyldisilazane (5 ml), chlorotrimethylsilane (50 μl) and dichloromethane (25 ml) and heated to reflux for 20 h. After cooling to ambient temperature, a solution of triethylamine (4.4 ml, 31.8 mmol) and dichloromethane (20 ml) was added. This solution was added to a cooled (−15 °C) solution of acryloyl chloride (2.5 ml, 30.3 mmol) and dichloromethane (50 ml) via a cannula within 2 h. The solution was stirred at room temperature overnight. 4,4′-sulfonylbis(methylbenzene) (500 mg) was added and the reaction mixture was concentrated by rotary evaporation and filtered. Then 1-methylpyrrolidin-2-one (10 ml) was added. The product was isolated as colorless oil via fractionated vacuum distillation. Yield: 4.8 g (73.9%) $T_m = 13$ °C, $[\alpha]_D^{25} + 68.9°$ (6.6 mg/ml, $CHCl_3$), ^{1}H NMR (C_6D_6): δ 6.41 (dd, 1H, $J = 17.0$, 1.9 Hz, –CH=CH_2), 6.39 (s, 1H, –NHCO–), 6.01 (dd, 1H, $J = 17.0$, 10.2 Hz, –CH=CH_2), 5.27 (dd, 1H, 10.2, 1.9 Hz, –CH=CH_2), 4.11 (tdd, 1H $J = 5.7$, 4.7, 3.8 Hz, –NH–CH<), 3.57 (dd, $J = 10.0$, 3.8 Hz, –CH_2–O–), 3.52 (dd, 1H, $J = 10.0$, 4.7 Hz, –CH_2–O–), 1.64 (m, 1H, –CH_2CH_3), 1.48 (m, 1H, –CH_2CH_3), 0.89 (t, 3H, $J = 7.5$ Hz, –CH_3), 0.07 (s, 9H, –Si–$(CH_3)_3$) ppm. ^{13}C NMR (C_6D_6): δ 165.0 (–CONH–), 131.9 (–CH=CH_2), 125.6 (–CH=CH_2), 64.1 (–CH_2–O–), 52.4 (–NH–CH<), 24.5 (–CH_2CH_3), 10.7 (–CH_3), −0.6 (–Si–$(CH_3)_3$) ppm. ^{29}Si NMR (C_6D_6): δ 17.9 ppm. IR (substance): 3434 (O=C<); 3277, 3069 (s, –NH–); 2963, 2902, 2878 (C–H); 1657 (O=C<); 1627 (>C=C<); 1549 (O=C<); 1252, 1113, 876, 842, 748 (–O–Si–$(CH_3)_3$) cm^{-1}.

2.5. Synthesis of N-(1-(trimethysilyloxy)butan-2-yl)acrylamide (R,S-TMSBA)

The synthesis was carried out starting from a racemic 2-Aminobutan-1-ol according to the preparation of R-TMSBA. The product was isolated as partly crystallizing oil via vacuum distillation. Yield: 1.5 g (23%) $T_m = 13$ °C.

2.6. Synthesis of poly-(R)-N-(1-(trimethylsilyloxy)butan-2-yl)acrylamide (P-R-TMSBA)

Typical procedure. R-TMSBA (250 mg) and the photoinitiator irgacure 184 (2.5 mg, 1 wt%) were dissolved in ethyl acetate (1 ml). The mixture was irradiated in a UV reactor (Heraflash, Heraeus Kulzer, Hanau, Germany) for 4 × 180 s. The solvent was evaporated under reduced pressure. T_g: 37 °C, $[\alpha]_D^{25} + 22.5°$ (c: 25 mg/ml, ethyl acetate), ^{1}H NMR ($CDCl_3$): δ 3.79 (m, 2H, –CH_2–O–), 3.56 (m, 1H, –NH–CH<), 2.01 (m, 1H, >CH–CO), 1.47 (m, 2H, –CH_2–), 1.39, 2H, (–CH_2CH_3), 0.87 (s, 3H, –CH_3), 0.08 (s, 9H, –Si$(CH_3)_3$) ppm. ^{13}C NMR ($CDCl_3$): δ 174.9 (–CONH–), 63.7 (–CH_2–O–), 52.0 (–NH–CH<), 43.6, 42.4 (>CH–CO), 36.2 (broad, –CH_2–), 24.2 (–CH_2CH_3), 10.6 (–CH_3), 1.3 (–Si–$(CH_3)_3$) ppm.. ATR-FT-IR: 3255 (>NH); 2953, 2866, (C–H); 1643, 1530 (O=C<); 1248, 1079, 866, 833, 744 (C–O–Si$(CH_3)_3$) cm^{-1}.

2.7. Synthesis of poly-(R)-N-(1-hydroxybutan-2-yl)acrylamide (P-R-HBA)

Typical procedure. R-TMSBA (522.3 mg) and the photoinitiator irgacure 184 (5.2 mg, 1 wt%) were dissolved in ethyl acetate (1 ml) (see Table 1). The mixture was irradiated in a UV reactor (Heraflash, Heraeus Kulzer, Hanau, Germany) for 4 × 180 s. The solvent was evaporated under reduced pressure. The residue was dissolved in a mixture of THF/aqueous HCl (THF: 0.1 M HCl, 90:10 vol%) and then dialyzed in the same solvent using a cellulose membrane with a molecular weight cutoff of 1000 g/mol. The solvent was changed every day. After four days the solvent was changed to a THF/water mixture (THF:water 90:10 vol%) and the dialysis was continued for another 24 h. The isolated polymer was dried in vacuo for 24 h. Yield: 317.7 mg, 91%. T_g: 59 °C, $[\alpha]_D^{25} + 12.8°$ (7.3 mg/ml MeOH), ^{1}H NMR (MeOD): δ 7.88 (s, 1H, –NHCO–), 3.97–3.01 (m, 3H, –CH_2–O–, –NH–CH<), 2.33–0.90 (m, 5H, –CH_2CH_3, –CH_2–, >CH–NH–), 0.84 (s, 3H, –CH_3) ppm. ^{13}C NMR (MeOD): δ 177.3 (–CONH–), 64.7, 63,6 (–CH_2–O–), 54.3 (>CH–NH–), 45.1, 43.7, (>CH–CO), 37.3 (broad, –CH_2–), 25.0 (–CH_2CH_3), 11.3 (–CH_3), ppm. ATR-FT-IR: 3264

Table 1
Synthesis of P-HBA polymers.

	TMSBA [mg]	$m_{irgacure184}$ [mg]	EA [μl]
1	250	2.5	500
2	250	2.5	1000
3	250	2.5	2000
4	250	12.5	1000
5	250	25.0	1000

(>NH, –OH); 2962, 2927, 2869 (C–H); 1636, 1543 (O=C<); 1051 (C–O) cm^{-1}.

2.8. Hydrolysis of P-R-TMSBA to poly(acrylic acid)

P-R-TMSBA (1 g) was dissolved in aqueous HCl (2 M, 15 ml) and toluene (3 ml) and heated to reflux for 48 h. The residue was dialyzed in warm water (50 °C) using a cellulose membrane with a molecular weight cutoff of 1000 g/mol for 4 days. The water was replaced every day. The remaining poly(acrylic acid) solution was washed with toluene (10 ml) and the solvent was evaporated under reduced pressure. The tacticity was determined by ^{1}H NMR spectroscopy [35,36].

2.9. Determination of the lower critical solution temperature (LCST)

The polymers (5 mg) were dissolved in distilled water (5 ml) with the aid of sonication and were stored at 4 °C for 4 days. The P-R-HBA polymers completely dissolved at this concentration. The racemic P-R,S-HBA polymers were not completely soluble. The samples were filtered through a PTFE membrane (Sartorius, Minisart SRP 4, 0.45 μm) before the measurements. The lower critical solution temperature was detected by the temperature dependent transmission (500 nm) of the sample with the Analytik Jena UV–vis spectrophotometer Specord S 600 equipped with a peltier element with a heating rate of 0.1 K/min within the range of 22 °C–32 °C.

2.10. Synthesis of the amphiphilic conetworks P-R-HBA-l-PDMS$_{1.1}$

A monomer mixture (80 μl) according to Table 2 containing PDMS$_{1.1}$ with a molecular weight of 1150 g/mol, R-TMSBA, and the photoinitiator irgacure 184 was poured on a glass slide. A second glass slide coated with a PP adhesive tape and two additional stripes as spacers were pressed atop. The monomer mixture was photopolymerized in a commercially available UV reactor (Heraflash, Heraeus Kulzer, Germany) for 4 × 180 s. The glass slides were separated and the polymer was removed from the adhesive tape. The network was incubated twice in a tetrahydrofuran/water mixture (50:50 vol/vol) overnight. Finally the conetwork was washed in water overnight, air dried on a PTFE sheet and subsequently vacuum dried.

2.11. Synthesis of the amphiphilic conetworks P-R-HBA-l-PDMS$_{5.6}$

The networks were synthesized similarly to the P-R-HBA-*l*-PDMS$_{1.1}$ conetworks with the exception that a cosolvent, ethyl acetate (1.1 mL per 1.0 mL of the monomer mixture) was added because the PDMS$_{5.6}$(MA)$_2$ macromonomer with a molecular weight of 5620 g/mol was not sufficiently soluble in R-TMSBA.

Table 2
Synthesis of amphiphilic conetworks.

PDMS content [wt%]	V_{TMSBA} [μl]	V_{PDMS} [μl]	$m_{irgacure184}$ [mg]	EA [μl]
80	60.0	147.0	1.0	235
70	90.0	128.7	1.1	248
60	120.0	110.3	1.1	262
50	120.0	73.5	0.9	220
40	250.0	102.1	1.7	400
30	190.0	49.9	1.1	273
20	200.0	30.6	1.1	262

2.12. Synthesis of the racemic amphiphilic conetworks P-R,S-HBA-l-PDMS$_{1.1}$

The conetworks were synthesized similarly to the P-R-HBA-*l*-PDMS$_{1.1}$ conetworks with the exception that the monomer was heated until all crystals were molten prior use.

2.13. Sol content

The sol fraction was determined by extracting a freshly synthesized P-TMSBA-*l*-PDMS conetwork with dichloromethane for 28 h. The sol fraction was calculated as the ratio of the mass of the extractable mixture of polymer and monomer and the non-extractable network. The composition of the extractable fraction was calculated from the ^{1}H NMR spectrum in $CDCl_3$.

2.14. Swelling measurements

Swelling experiments at ambient or higher temperature were carried out by immersing a conetwork sample in an excess of distilled water and *n*-heptane, respectively. If appropriate, the temperature was controlled by heating with a block thermostat (Grant, UBD1). The sample dimensions were measured with a Motic SMZ-168 Binocular Microscope. The equilibrium volumetric degree of swelling *S* was calculated from:

Eq. (1) Equilibrium volumetric degree of swelling.

$$S = \frac{V_e}{V_0} \tag{1}$$

where V_e is the volume of the swollen and V_0 that of the dry sample. Temperature dependent swelling experiments between 2 °C and ambient temperature were carried out in a large excess of iced water allowing to heat to ambient temperature within 6 h. The sample dimensions were recorded with a digital camera.

2.15. Release measurements

The network samples (20 mg) were incubated in a solution of cinchona alkaloids (+)-cinchonin and (−)-cinchonidine (5 mL, 5 mg/ml) in chloroform overnight, carefully washed with chloroform and dried in vacuo. The concentration of *cinchona* alkaloids in the conetworks was determined by UV-absorbance at 317 nm. For releasing, a loaded conetwork (15 mg) was clamped in a stirred UV–vis cell filled with chloroform (2 ml). The release rate of the cinchona alkaloids was measured by the increasing absorbance at 317 nm.

3. Results and discussion

The Goal of this work was the synthesis and characterization of APCNs with a chiral hydrophilic phase. In order to synthesize such architecture, the approach of the copolymerization of a macromeric hydrophobic crosslinker with a hydrophilic monomer was chosen. As described by Ivan and Kennedy, the miscibility of these two compounds can be achieved by modification of the hydrophilic monomer with a hydrophobic TMS protecting group, which is cleaved after the polymerization procedure [3]. Since most APCN applications require their well-known nanophase morphology throughout the whole material, we chose photopolymerization as a fast procedure in order to avoid early separation of the formed polymers. A suited chiral monomer known from the literature is (1-hydroxymethyl) propyl-methacrylamide (HMPMA) [37]. Since we had trouble to obtain APCNs with methacrylate derivatives as

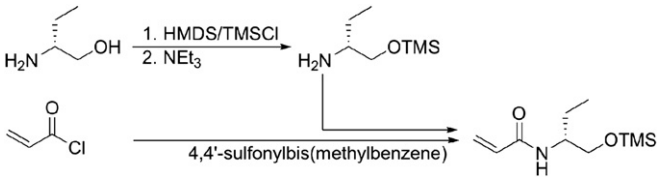

Fig. 1. Synthesis of (R)-*N*-(1-(trimethysilyloxy)butan-2-yl)acrylamide.

monomers in the past [29], we decided to synthesize the respective acrylamide derivative in its TMS-protected form.

3.1. Synthesis of (R)-N-(1-(trimethylsilyloxy)butan-2-yl)acrylamide (R-TMSBA)

The monomer R-TMSBA was synthesized in a one–pot reaction (see Fig. 1). First, the (R)-2-aminobutan-1-ol was converted into the protected (R)-1-(trimethylsilyloxy)butan-2-amine by a silylation with an excess of hexamethyldisilazane and a catalytic amount of TMSCl in dichloromethane under reflux. A silylation of the amino group was not observed. The subsequent reaction of the (R)-1-(trimethylsilyloxy)butan-2-amine with acryloyl chloride resulted in the monomer R-TMSBA. A catalytic amount of 4,4′-sulfonylbis(methylbenzene) was added as a radical scavenger. Furthermore, this radical scavenger reduced the aggregation of the acrylamide derivative molecules which greatly simplified the subsequent vacuum distillation. Pure R-TMSBA in an overall yield of 74% was obtained. NMR confirmed the identity of R-TMSBA and the chirality was proven with optical rotation measurements (see experimental section). The respective S-TMSBA was prepared under the same conditions and showed similar properties. The racemic R,S-TMSBA was synthesized in the same manner. Unfortunately the tendency of the racemic derivative to crystallize resulted in a significantly lower yield compared to R-TMSBA. The chiral monomers R-TMSBA and S-TMSBA show a distinct melting point of 13 °C. In contrast R,S-TMSBA seems to be polymorph with a melting point of 13 °C followed by a melting zone which expands to 39 °C, probably due to the formed diasterimeric R,S-dimers. In order to analyze such a dimerization, the ATR-FT-IR spectrum of the respective monomers was recorded (in Fig. 4). The downshift of the transoid valence vibration of the N–H bond to 3277 cm^{-1} indicates that the monomer R-TMSBA forms hydrogen bonds. Moreover the valence vibration of a cisoid N–H bond (combined with an amide II harmonic) at 3069 cm^{-1} shows that R-TMSBA in substance has a propensity to intermolecular H-Bond assisted dimerisation to some extent [38]. The same conclusion can be drawn for R,S-TMSBA with the difference that the formed hydrogen bonds are more stable as indicated by the downshift of the transoid valence vibration of the N–H bond to 3248 cm^{-1}. This might explain the different thermal properties of the chiral monomers and the respective racemate (Fig. 2).

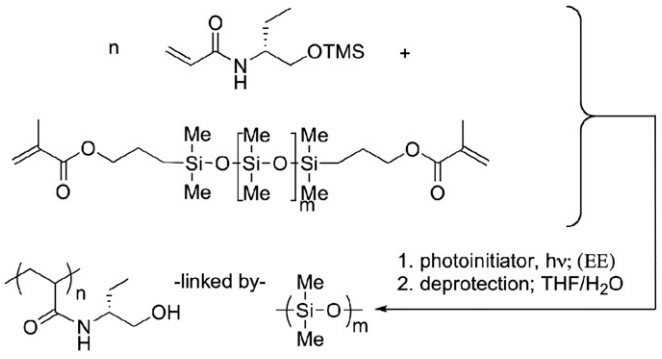

Fig. 2. Synthesis of chiral amphiphilic conetworks.

Having established the chemical structure of the monomers, we chose to synthesize the respective homopolymers via photopolymerization to explore the properties of the potential hydrophilic network phase and to see the influence of the polymerization procedure to possible racemization. It was expected that the polymerization of R-TMSBA would result in macromolecules with the same properties as those derived from the respected S-derivative. Thus, only polymers from R-TMSBA and R,S-TMSBA were investigated. First R-TMSBA was polymerized under conditions typical for APCN synthesis. The isolated polymer exhibited an optical rotation of +22.5° in ethyl acetate. The TMS group of the hydrophobic poly-(R)-*N*-(1-(trimethylsilyloxy)butan-2-yl)acrylamide (P-R-TMSBA) was then cleaved with a 1:1 (vol./vol.) mixture of THF and 0.1 M aqueous HCl. The resulting polymer poly-(R)-*N*-(1-hydroxybutan-2-yl)acrylamide (P-R-HBA) was still optically active, showing an optical rotation of +12.8°. As described by Aoki [37], the respective poly(methacrylamide) derivative exhibits an LCST in aqueous solution. Although the polymer backbone is more flexible, we suspected that P-R-HBA might show a similar behavior in aqueous solution.

To test the synthesized polymer P-R-HBA regarding its LCST, the macromolecule was dissolved in water and the light-transmittance of the solution was recorded with a UV–vis spectrophotometer at different temperatures. It was found that the polymer exhibits a very narrow LCST at 25 °C. The lower critical solution temperature (LCST) phenomenon is attributed to the entropy increase from the loss of hydrophobically bonded water upon heating and is well documented for polymers like PNIPAM, the chiral poly(*N*-acryloyl-L-proline methyl ester [39] or *N*-(L)-(1-hydroxymethyl) propylmethacrylamide) [37,40]. The interrelation of the LCST and the regularity of the polymer have been reported in the case of stereoregular PNIPAM [41]. In order to explore the influence of molecular weight and optical activity to the LCST of P-HBA, a series of polymers starting from R-HBA as well as from R,S-HBA was prepared varying the initiator/monomer ratio as well as the amount of the solvent ethyl acetate (see Table 1).

As seen in Table 3 and Fig. 3, the LCST of P-R-HBA (23.7–26.8 °C) is nearly independent on the molecular weight within a range of 97–164 kDa (M_n). The comparison of the transmittance in the heating and cooling cycle (Fig. 3) indicates that the polymers do not exhibit a pronounced hysteresis. The same is true for the non-chiral polymer P-R,S-HBA which exhibits the same LCST (24.8–26.3 °C) as its chiral analogue. Obviously the lateral chirality does not influence the LCST either. A notable observation is the partial resolubilization of the racemic P-R,S-HBA at 29 °C.

Another important influence on the LCST of polymers is the stereoregularity of the latter [41]. Chiral side groups are reported to control the tacticity of poly(acrylate) derivatives. Porter et al. [36]

Table 3
Synthesized homopolymers P-HBA.

	M_w [1000 g/mol]	M_n [1000 g/mol]	M_w/M_n [1000 g/mol]	T_g [°C]	T_m [°C]	LCST [°C]
1R	91	146	1.6	58.5	–	23.7
2R	56	116	2.1	–	–	24.8
3R	53	108	2.0	58.5	106.9	25.1
4R	38	97	2.5	56.0	103.6	25.7
5R	78	164	2.1	62.6	106.4	25.2
1 rac	101	263	2.6	57.6	–	24.8
2 rac	80	160	2.0	58.3	–	25.0
3 rac	53	137	2.6	58.4	–	26.3
4 rac	54	153	2.6	58.9	–	25.4

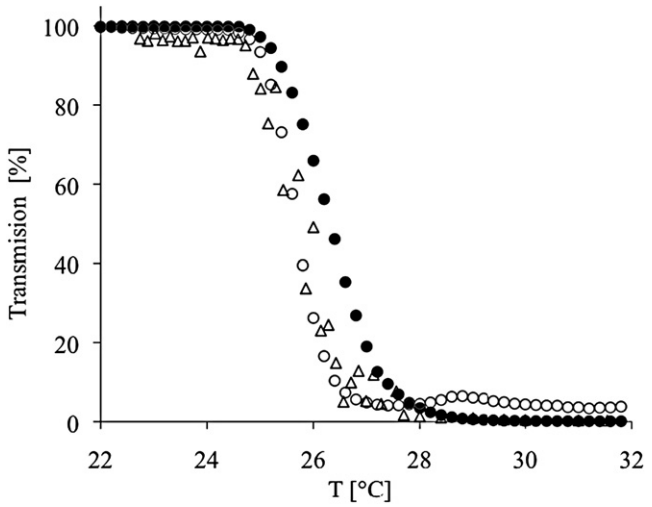

Fig. 3. Temperature dependent transmission of a polymer solution in water (1 mg/ml). P-R-HBA (3 R) ● heating cycle, △ cooling cycle and ○ P-R,S-HBA (3 rac) heating cycle.

described the synthesis of a highly isotactic poly(acrylamide) by the introduction of chiral oxazolidine residues yielding up to 92% isotactic polymers. In order to explore the stereoregularity of the synthesized P-R-HBA and P-R,S-HBA they were hydrolyzed to yield the respective poly(acrylic acid)s which were then studied with ^{1}H NMR. According to literature [35,36] the methylene protons of poly(acrylic acid) are sensitive to the diad stereochemistry of the backbone of the polymer and have been identified before. The downfield peak at 2.15 ppm can be related to an isotactic diad. The next upfield peak (1.85 ppm) represents the syndiotactic diad which is partially overlapping the second isotactic peak at 1.60 ppm. The overlap of the isotactic and syndiotactic peaks hamper the analysis of the tacticity of the polymer backbone. Monjol [35] suggested the following formula which was used for the calculation of the isotactic content of the polymer.

Calculation of the isotactic content of the polymer via ^{1}H NMR:

$$\%i = \frac{2\int H_{\text{isotactic, downfield}}}{\int H_{\text{isotactic, downfield}} + \int H_{\text{syndiotactic}} + \int H_{\text{isotactic, upfield}}} \quad (2)$$

An isotactic content of 44% was achieved for all P-R-HBA. The polymerization of R,S-TMSBA in substance (1 rac) resulted in a 46% isotactic polymer and the polymerization of a 581 μmol/l solution in ethyl acetate in a 33% isotactic polymer (4 rac). Thus the isotactivity of the P-HBAs could be varied from 33% to 46%. Since the polymers show similar LCST it can be concluded that the stereoregularity does not significantly influence this temperature for the synthesized P-HBAs macromolecules.

The glass transition temperatures of the polymers are important to the mechanical and swelling properties of any P-HBA containing material. The chiral as well as the racemic polymers show T_g values in a range of 56–62 °C and are thus independent on the pendent chirality. Furthermore the chiral polymers 3R, 4R and 5R are partly crystalline and exhibit a melting point between 103 and 107 °C. All P-R-HBA samples are soluble in water, methanol, and ethanol. They are swellable in DMSO and chloroform and insoluble in hydrocarbons and acetone.

Altogether the synthesized P-HBA are polymers with a T_g and an LCST in water that are independent on their molecular weight, their stereoregularity, and their chirality. They are further soluble and swellable in polar solvents and not solvated by non-polar solvents.

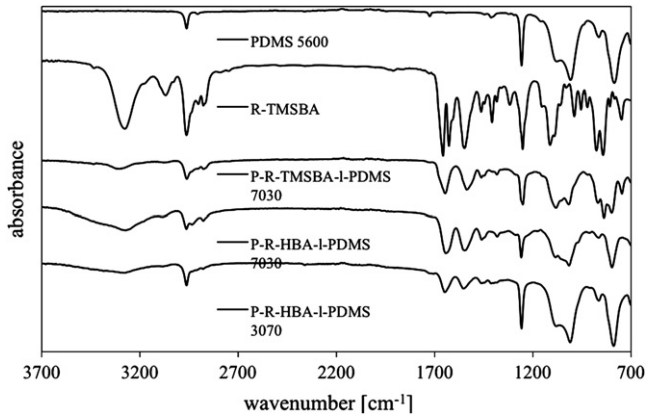

Fig. 4. ATR-FT-IR spectra of $PDMS_{5.6}(MA)_2$, R-TMSBA, P-R-TMSBA-*l*-$PDMS_{5.6}$ 73/27, P-R-HBA-*l*-$PDMS_{5.6}$ 73/27 and P-R-HBA-*l*-$PDMS_{5.6}$ 30/70.

This makes these polymers excellent candidates as chiral, hydrophilic, and even thermosensitive phases in APCNs. Such conetworks will allow insights in the phase behavior of two independently swelling nanoseparated polymer phases. Further, they might be universal and superior separation materials due to this unique controllable swelling.

3.2. Poly-(R)-N-(1-hydroxybutan-2-yl)acrylamide-l-poly-(dimethylsiloxane) (P-R-HBA-l-PDMS)

In order to prepare such APCNs we chose to photocopolymerize R-TMSBA with the established bitelechelic methacrylate-terminated poly(dimethylsiloxane) (PDMS) as macromolecular, hydrophobic crosslinker. In order to vary the crosslinking density at similar concentrations, PDMS with a molecular weight of 1150 g/mol ($PDMS_{1.1}$) and of 5620 g/mol ($PDMS_{5.6}$), respectively, was used. $PDMS_{1.1}$ is miscible with R-TMSBA and the network synthesis could be performed in bulk. To obtain a homogeneous mixture of $PDMS_{5.6}$ and R-TMSBA, ethyl acetate was used as inert cosolvent. Conetworks with a composition ranging from 84 to 20 wt% PDMS were synthesized. The conversion of the prepolymer solution into the homogeneous conetwork was monitored by IR spectroscopy. A complete conversion of the monomer was ensured by the disappearance of the 1624 cm^{-1} peak which is typical for carbon carbon double bonds. The homogeneous precursor networks were transformed into the amphipilic conetworks by cleaving the trimethylsilyl group using a mixture of THF and water (THF:H_2O, 50:50 vol/vol). The deprotection procedure was monitored via ATR-FT-IR spectroscopy as well (see Fig. 4). The comparison of the IR spectra of the homopolymers P-R-TMSBA and P-R-HBA reveals that washing with a mixture of THF and water (THF:H_2O, 50:50 vol%) overnight results in a complete disappearance of the peaks at

Fig. 5. Photograph of a P-R-HBA-*l*-$PDMS_{5.6}$ conetwork with a PDMS content of 49 wt%.

Table 4
Glass transition temperatures T_g of the APCNs.

PDMS content [wt%]	T_g [°C]			
	1100 [g/mol]		5600 [g/mol]	
70	73	−128	61	−125
60	74	−130	63	−123
50 (49)	76	−128	62	−126
40 (39)	74	−134	62	−125
30 (27)	74	−131	65	−127

743 cm^{-1}, 832 cm^{-1}, 850 cm^{-1} and 1247 cm^{-1}. These peaks can be attributed to the TMS protecting group. The cleaving of the silyl-ether results in a shift of the 1079 cm^{-1} peak to 1049 cm^{-1}. The strong absorbance at 1247 cm^{-1} is not suitable to monitor the deprotection procedure of the network. The comparison of the IR spectra of the $PDMS_{5.6}$–crosslinker and P-R-TMSBA indicates that this peak is overlaid by a strong absorbance of PDMS. The shift of the 1079 cm^{-1} is also concealed by a strong peak of the PDMS. Only the peaks at 743 cm^{-1} and 832 cm^{-1} are appropriate to monitor the cleaving of the TMS group. Comparison of the spectra of the homogeneous network P-R-TMSBA-*l*-$PDMS_{5.6}$ 73/27 and the amphiphilic conetwork P-R-HBA-*l*-$PDMS_{5.6}$ 30/70 shows that the washing of the network samples with the THF/water mixture for two days results in a complete deprotection. The varying compositions of the conetworks P-R-TMSBA-*l*-$PDMS_{5.6}$ 73/27 and P-R-HBA-*l*-$PDMS_{5.6}$ 30/70 are visualized in the relative magnitude of the PDMS related 779 cm^{-1} and 1257 cm^{-1} peaks and the amide I and II peaks of P-R-HBA at 1630 cm^{-1} and 1535 cm^{-1}.

Finally, transparent membranes with a thickness in the range of 20–70 μm were obtained (see Fig. 5). The transparency is an indicator that no macroscopic phase separation occurred, i.e., gelation was faster than the separation of the formed polymers.

In order to verify the composition of the networks and the quality of network formation, the sol fraction was determined by extracting the protected conetworks with dichloromethane for 24 h. The sol fraction was found to be 7 ± 2 wt% for the network P-R-HBA-*l*-$PDMS_{5.6}$ with a PDMS content of 30 wt%. The sol fraction for a network containing 70 wt% PDMS was 7 ± 1 wt%. This is comparable to the achieved sol fraction in similar networks [42]. The ^1H NMR of the extractable part of an APCN with a PDMS content of 30 wt% reveals that the sol fraction has a composition of 1 wt% not converted R-HBA, 34 wt% of oligomeric P-R-HBA and 65 wt% of PDMS. This results in a final composition of 73 wt% P-R-HBA and 27 wt% PDMS. The composition of the sol fraction of the network with 70 wt% PDMS was determined to be 9 wt% non-reacted R-HBA, 23 wt% of oligomeric P-R-HBA and 68 wt% of PDMS. The corrected composition of the P-R-HBA-*l*-$PDMS_{5.6}$ conetwork diverts less than 0.2 wt% from the starting concentration. The high content of PDMS in the sol fraction can be explained by an insufficient functionalization of the silanol terminated PDMS. The sol fraction of a P-R-HBA-*l*-$PDMS_{1.1}$ network with 50 wt% PDMS was found to be as low as 1.5 wt%. Altogether, the network formation is nearly ideal in all cases and the composition of the final APCNs is – within the experimental error – that of the starting monomer mixture.

According to their incompatibility, P-R-HBA and PDMS are expected to phase separate on the nanoscale. One important indicator of such a separation is that each polymer nanophase exhibits its own independent glass transition temperature. As shown with DSC, all conetworks have two distinct T_g values (Table 4). The P-R-HBA-*l*-$PDMS_{1.1}$ conetworks have a T_g of around −130 °C and a second T_g around 74 °C. The T_g values can be related to those of the homopolymers PDMS (−127 °C [43]) and P-HBA (59 °C). The P-R-HBA-*l*-$PDMS_{5.6}$ networks exhibit similar thermal properties with glass transition temperatures of around −125 °C which can be related to PDMS and one of around 63 °C identified as the T_g of P-HBA. The T_g values seem to be independent on the composition of the conetworks. Interestingly, the T_g of the conetwork with the long crosslinker $PDMS_{5.6}$ exhibits a T_g of the P-R-HBA phase close to that of free polymer, while the conetwork with the shorter crosslinker $PDMS_{1.1}$ shows an T_g value that is about 11 K higher. An explanation for this could be that in the latter case the PDMS terminating methacrylate groups form a statistical copolymer with the R-HBA monomers which result expectedly in a T_g value between the two of P-R-HBA and poly(methacrylate). In the case of the longer crosslinker the content of methacrylate is very low and is not influencing the T_g of the resulting copolymer.

Atomic force microscopy in the phase mode is a powerful tool to visualize polymer nanophase morphologies, because this method can distinguish between hard and soft phases that do not show any other differences. The measurements were performed on cryocuts of the APCNs and represent the bulk morphology of the conetworks. The softer PDMS phase appears dark and the harder P-R-HBA appears bright. The AFM images shown in Figs. 6 and 7 show a morphology typical for amphiphilic conetworks [3]. Unlike classical block copolymer morphologies a long-range periodicity is not observable.

However, all AFM images of the P-R-HBA-*l*-$PDMS_{1.1}$ conetworks in compositions ranging from 20 to 80 wt% PDMS have nearly no contrast between the two phases. This indicates that the polymer segments are too short to afford a block copolymer-like phase separation between P-R-HBA and PDMS, i.e., the conetworks are more alike hydrophilic polymers crosslinked by a low molecular weight compound. Since the photoinitiated free radical polymerization ensures a fast gelation, the found morphology could be explained by "freezing" the structure of the pre polymer solutions upon crosslinking. Despite the fact that phase separated conetworks were previously obtained from solvent free

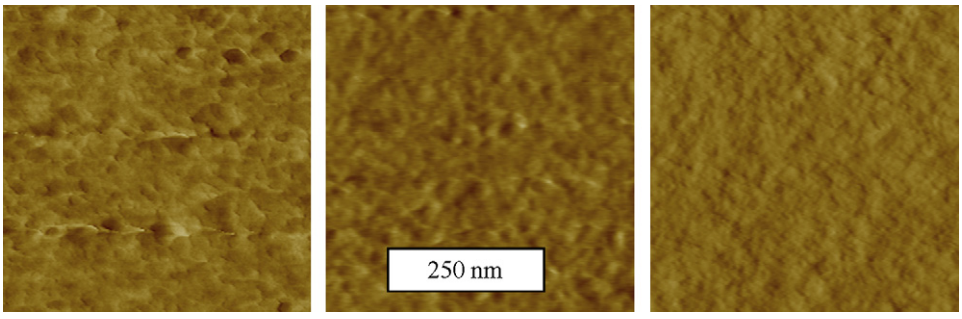

Fig. 6. AFM phase mode images of P-R-HBA-*l*-$PDMS_{1.1}$ conetworks with 80, 50 and 20 wt% PDMS content (left to right).

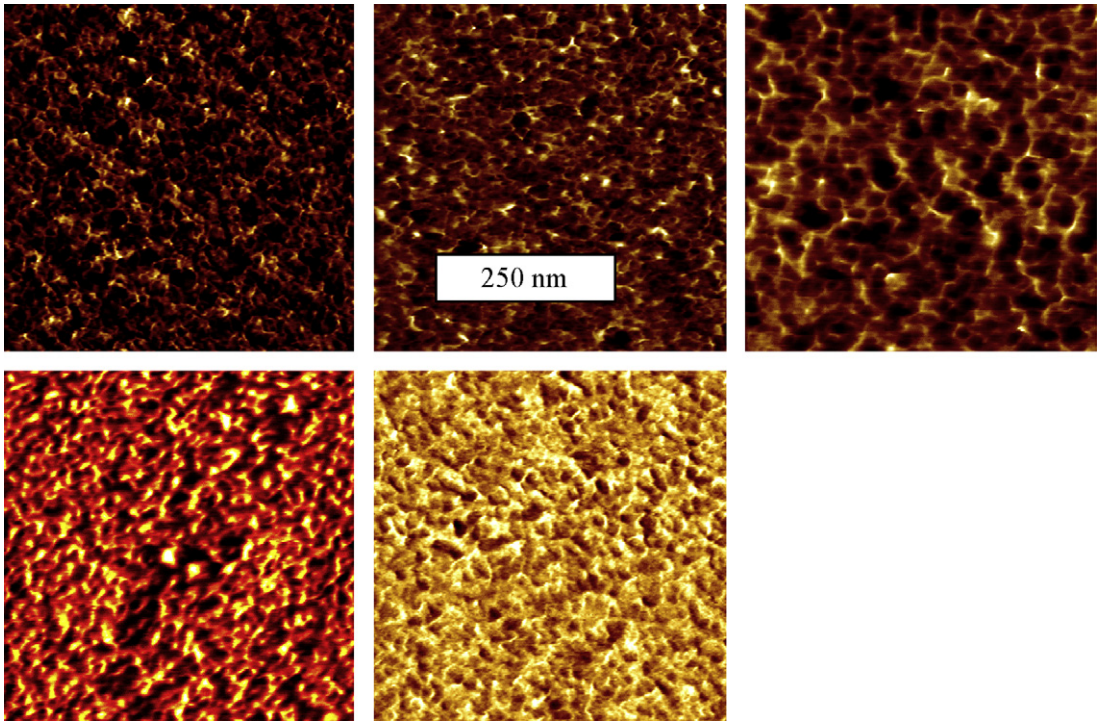

Fig. 7. AFM phase mode images of P-R-HBA-*l*-PDMS$_{5.6}$ conetworks with 80, 70, 60 (top, left to right), 49 and 27 wt% (bottom, left to right) PDMS content.

copolymerisation with PDMS macro crosslinkers [3,29], the absence of a solvent may contribute to the lacking of a phase separation.

AFM measurements on the P-R-HBA-*l*-PDMS$_{5.6}$ conetworks show two distinct polymer nanophases. The images of the P-R-HBA-*l*-PDMS$_{5.6}$ conetwork with 70 and 80 wt% PDMS are dominated by the nodular 10–16 nm sized PDMS domains. It is pervaded by slender 10–20 nm wide branches of the brighter (harder) P-R-HBA. The structure of the P-R-HBA-*l*-PDMS$_{5.6}$ networks with 49%–60 wt% PDMS are bicontinuous. The spherical PDMS domains with a size of some 12 nm are interconnected. Likewise the brighter P-R-HBA phase generates a netlike structure in the PDMS matrix with a domain size of 6–10 nm. The structure of the P-R-HBA-*l*-PDMS$_{5.6}$ conetwork with 27 wt% PDMS is dominated by a bright P-R-HBA net. The spherical PDMS domains of some 10 nm in size are embedded in the P-R-HBA matrix. AFM suggests that the PDMS spheres are connected to some extend.

The swelling in orthogonal solvents is one of the main characteristics of APCNs. A very intriguing possibility is the independent swellability of the two phases. This is still a proposed phenomenon that has not been shown for most APCNs. In order to get a better insight in the composition of the investigated conetworks, the average M_c was calculated according to Eq. (3). As seen in Table 5, the two PDMS crosslinkers afford a significantly different M_c of the P-R-HBA phase at the same composition in terms of wt%. This has affected the T_g of the latter as shown above and should affect the swelling properties as well.

Relation of the $M_{c,P\text{-}R\text{-}HBA}$ and the molecular weight of the PDMS crosslinker [1]:

$$M_{c,PHBA} = \frac{1}{2}\frac{w_{PHBA}}{w_{PDMS}} M_{n,PDMS} \quad (3)$$

It was expected that water swells exclusively the P-R-HBA phase while *n*-heptane swells the PDMS phase. The swelling of the P-R-HBA-*l*-PDMS membranes in these two solvents was determined by measuring the dimensions of the networks prior and after soaking the materials in the respective liquid. After immersing the APCNs in *n*-heptane and water, respectively, transparent gels were obtained.

The degree of swelling of the networks in *n*-heptane in dependence on their composition is shown as full symbols in Fig. 8 and the swelling in water at room temperature is presented as empty symbols in the same Figure. Obviously, the two conetworks have completely different swelling characteristics.

The APCNs with the short macromeric crosslinker PDMS$_{1.1}$ start to significantly swell in *n*-heptane at the composition of some 20 wt% PDMS. Increasing the PDMS content results in higher swelling degrees, which corresponds to the amount of poly(dimethylsiloxane). The swelling reaches a maximum at 60 wt% PDMS and decreases with higher silicone contents. This is a typical behavior of a homogeneous conetwork based on a hydrophilic polymer crosslinked with a hydrophobic low molecular weight compound [44,45]. Obviously, the conetworks swell comparable to

Table 5
Calculated molecular weight per crosslinked unit M_c and n_c the average number of monomer units between cross-links of P-R-HBA depending on the composition of the networks and the molecular weight of the macro crosslinker PDMS.

w_{PDMS}	$M_{cP\text{-}R\text{-}HBA}$		n_c	
	1100 [g/mol]	5620 [g/mol]	1100 [g/mol]	5620 [g/mol]
0.9	61	312	0.4	2.2
0.8	138	703	1.0	4.9
0.7	236	1204	1.6	8.4
0.6	367	1873	2.6	13.1
0.5	550	2810	3.8	19.6
0.4	825	4215	5.8	29.4
0.3	1283	6557	9.0	45.8
0.2	2200	11,240	15.4	78.5
0.1	4950	25,290	34.6	176.6

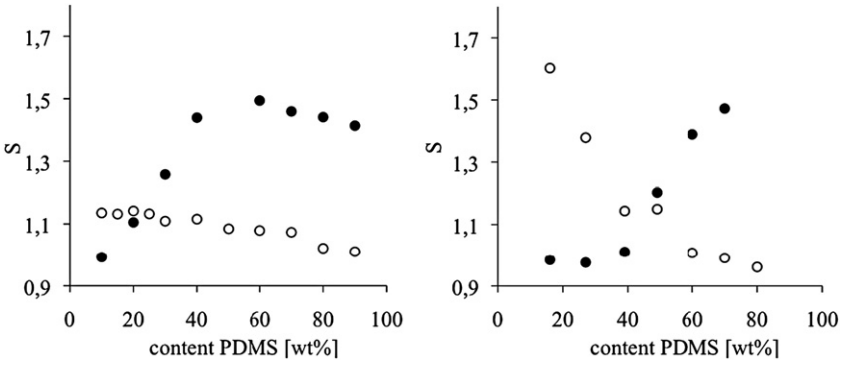

Fig. 8. left: Swelling of P-R-HBA-*l*-PDMS$_{1.1}$ in ●: *n*-heptane and ○: water, right: Swelling of P-R-HBA-*l*-PDMS$_{5.6}$ in ●: *n*-heptane and ○: water.

a copolymer mixture und do not show a phase separation that enables the hydrophobic PDMS phase to swell independently from the hydrophilic P-R-HBA phase. This is supported by the AFM images of the conetworks, which reveal the lack of phase separation (cf. Fig. 6). Further, the higher T_g values of P-R-HBA in the conetwork indicate the existence of statistical copolymer phases as well. The decrease in swelling above 60 wt% of PDMS can be explained by an increasing crosslinking density. The swelling in water supports the conclusion that the polymers are not sufficiently phase separated. Surprisingly, the P-R-HBA does not swell to more than 20 vol% in all investigated P-R-HBA-*l*-PDMS$_{1.1}$ compositions.

In contrast to the findings above, the swelling of P-R-HBA-*l*-PDMS$_{5.6}$ in *n*-heptane starts at 50 wt% PDMS although the longer PDMS crosslinker affords a lower crosslinking density. According to the AFM images in Fig. 7, the APCNs consist of a hard matrix with embedded PDMS spheres. The acrylamide matrix does not swell in *n*-heptane and due to the fact that its T_g is above room temperature the solvent cannot easily permeate the matrix. Thus, the acrylamide phase forms a rigid solvent barrier that does not allow swelling of the PDMS even at a content of 40 wt%. However, the PDMS phase starts to be interconnected at 50 wt% PDMS allowing the *n*-heptane to swell this phase of the conetwork. Further increasing of the PDMS content affords an even greater swelling of the hydrophobic phase. A PDMS content of 80 wt% leads to a dramatic increase in swelling up to 284% (data point not shown in Fig. 8, right). This degree of swelling is comparable to a similar PHEA-*l*-PDMS$_{5.2}$ conetwork [3] and in both cases the AFM images revealed that the acrylamide phase is no longer interconnected at this composition. In consequence, the PDMS phase is not limited in swelling by the non-swelling acrylamide conetwork any more.

The swelling in water shows a similar but inverse characteristic compared to the swelling in *n*-heptane. This indicates that the water exclusively swells the P-R-HBA phase.

Comparing the swelling characteristics of the P-R-HBA-*l*-PDMS conetworks with different crosslinker lengths and combining them with the AFM images and the DSC measurements gives a clear picture of the effect that morphology has on the properties of APCNs. It further shows that the minimal length of the crosslinker for obtaining a nanophase separation in an APCN is more than 1100 g/mol and that two different T_g values in a clear polymer conetwork are not sufficient to predict a nanophase separation.

Having established the separate swellability of the two polymer phases of the P-R-HBA-*l*-PDMS$_{5.6}$ it was then investigated how the swelling degree of the conetworks reacts to temperature. It was expected that the conetwork shows an abrupt change in dimensions at the LCST of P-R-HBA in water, which is the case for most thermosensitive networks in the literature [46,47]. Furthermore, a dramatic change can be predicted at the T_g of P-R-HBA when swelling the APCNs in hydrocarbons.

In order to examine the effect of temperature on the swellability of the conetworks in water, the equilibrium degree of swelling *S* was measured at different temperatures starting at 2 °C (see Fig. 9). In contrast to the swelling data above, the values for *S* are recorded after shorter swelling intervals and do not represent equilibrium swelling data. Thus, they are not comparable to the data shown in Fig. 3.

In the case of the conetwork P-R-HBA-*l*-PDMS$_{5.6}$ with a P-HBA content of 80 wt% the increase of the temperature results in a linear decrease in the degree of swelling *S* from 2.6 at 2 °C to 1.1 at 40 °C. The conetwork P-R-HBA-*l*-PDMS$_{5.6}$ with a PDMS content of 49 wt% shows the same behavior with the difference that the degree of swelling is about 1.5 at 2 °C and around 1.1 at 40 °C. The comparison of the heating cycle with the cooling cycle of the P-R-HBA-*l*-PDMS$_{5.6}$ with a PDMS content of 20 wt% reveals that the network undergoes a slight thermal hysteresis. The temperature/swelling hysteresis in water of the APCN with a PDMS content of 49 wt% is less pronounced.

In order to explore if the found linear temperature sensitivity over a broad temperature range is due to the phase separation of the APCNs, the not phase separated conetwork P-R-HBA-*l*-PDMS$_{1.1}$ with a P-R-HBA content of 80 wt% was investigated as well. According to Table 1, the crosslinking density of this conetwork is

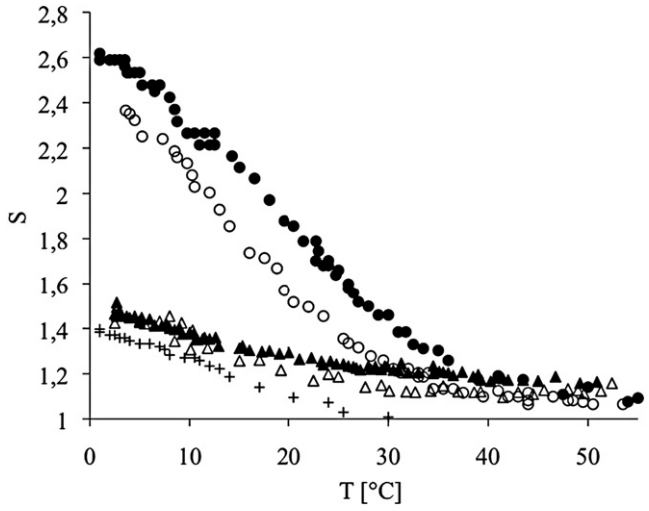

Fig. 9. Temperature dependent swelling of APCNs in water. P-R-HBA-*l*-PDMS$_{5.6}$ 84/16 ● heating cycle, ○ cooling cycle, P-R-HBA-*l*-PDMS$_{5.6}$ 51/49 ▲ heating cycle, △ cooling cycle, P-R-HBA-*l*-PDMS$_{1.1}$ 80/20 + heating cycle.

comparable to that of the respective P-R-HBA-*l*-PDMS$_{5.6}$ with some 40–50 wt% P-R-HBA content. Surprisingly, the conetwork shows a linear decrease of swelling by an increase of the temperature as well, even in the same range as the respective APCN. In contrast to the latter, the conetwork crosslinked by PDMS$_{1.1}$ decreases its swelling to $S = 1.00$, which can be read as no swelling at all, while the conetwork crosslinked by the longer PDMS shows some 10% volume swelling even at 40 °C. Additionally, the swelling behavior is fully reversible and does not show a hysteresis (data not shown). These findings indicate that the linear temperature sensitivity of the P-R-HBA-*l*-PDMS in water is most likely due the crosslinking with a hydrophobic, low T_g polymer. A nanophase separation does not seem necessary for the effect.

Altogether, all investigated conetworks do not exhibit a sharp transition in swelling in water at 25 °C, which would be expected because of the LCST behavior of the P-R-HBA but they showed a nearly perfect linear decrease in swelling over a temperature range of some 30 K. The reason for the linear decrease of swelling could be attributed to the statistical distribution of the hydrophobic comonomer PDMS within the P-R-HBA chains. The role of the low T_g PDMS crosslinker in the swelling is part of current investigations. However, the surprising linear temperature control over up to 250 vol% of the conetworks in a range of 30 K might be a very promising tool for using these membranes as smart materials in sensors and separation techniques.

While the temperature dependent swelling in water is apparently not hindered by the elastic PDMS crosslinker, the swelling of the PDMS phase should behave differently because in contrast to the poly(dimethylsiloxane), the P-R-HBA phase is below T_g and therefore rigid. It was expected that the swelling of the PDMS phase might therefore be dependent on the temperature near T_g.

In order to investigate this hypothesis, we measured the temperature dependent swelling of a series of P-R-HBA-*l*-PDMS$_{5.6}$ conetworks with different compositions in *n*-heptane (see Fig. 10). The swell ability of the conetwork sample with a PDMS content of 27 wt% is constant at $S = 1.02 \pm 0.02$ at ambient temperature. A strong increase of the swelling was observed near the glass transition temperature of the hydrophilic phase (≈ 59 °C). A second plateau with an S of 1.11 ± 0.02 is reached at 67 °C. The conetworks with a higher PDMS content exhibit a higher degree of swelling in *n*-heptane at ambient temperature. The APCN with a PDMS content

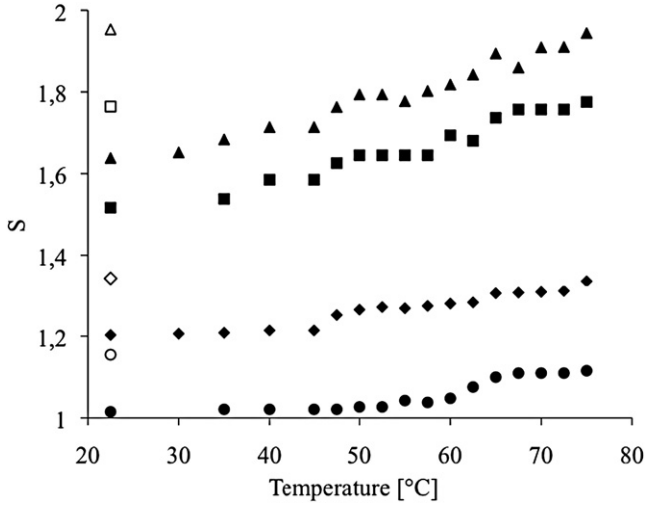

Fig. 10. Temperature dependent swelling of APCN in *n*-heptane. ● P-R-HBA-*l*-PDMS$_{5.6}$ 84/16, ◆ P-R-HBA-*l*-PDMS$_{5.6}$ 51/49, ■ P-R-HBA-*l*-PDMS$_{5.6}$ 40/60, ▲ P-R-HBA-*l*-PDMS$_{5.6}$ 30/70. After recooling open symbols.

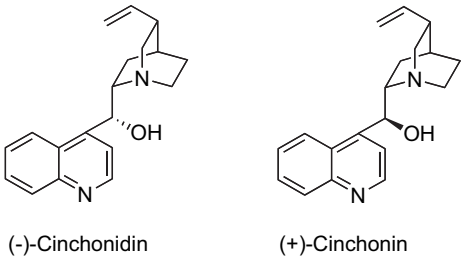

Fig. 11. Structures of the *cinchona* alkaloids.

of 49 wt% likewise shows a plateau at $S = 1.21 \pm 0.03$ around room temperature. The degree of swelling switches to become temperature dependent by heating the sample up over 50 °C and reaches $S = 1.33 \pm 0.04$ at 75 °C. The sample with a PDMS content of 70 wt% has expectedly the highest swell ability at ambient temperature with $S = 1.64 \pm 0.06$ and increases this linearly up to $S = 1.94 \pm 0.08$ at 75 °C.

In all cases, the temperature dependent swelling is not reversible by cooling the high temperature swollen conetwork samples to ambient temperature within 30 min and maintaining it for 2 days. The maintenance of the highly swollen state is accompanied by the restiffening of the stretched non-swollen hydrophilic P-R-HBA. These observations indicate that the swell ability of the APCNs in a PDMS selective solvent are not in its thermodynamic equilibrium until the temperature reaches the T_g of the second non-swollen phase. This is supported by the fact that the swelling degrees in *n*-heptane after heating above T_g are almost exactly that of a PHEA-*l*-PDMS$_{5.2}$ conetwork [3] which contains two polymer phases with T_g values below room temperature. This shows quite impressively that only the morphology and topology of the conetworks but not their chemical composition are responsible for their swelling properties in suited solvents.

The above demonstrated advantage of the polymer conetworks to separately swell in orthogonal solvents should enable the prepared membranes to separate racemates not only in water but also in organic solvents. In order to explore this, we chose to determine the interaction of the enantiomeric conetworks, P-R-HBA-*l*-PDMS$_{1.1}$ and P-S-HBA-*l*-PDMS$_{1.1}$, with the *cinchona* alkaloids (−)-cinchonidine and (+)-cinchonine in chloroform (see Fig. 11). All used conetworks contained 50 wt% of PDMS. First, the membranes were loaded by immersing them into the respective alkaloid chloroform solution overnight. The UV–vis detected loading of the networks already indicates selective interactions between alkaloid and the matrix via hydrogen bonds between the chiral poly (acrylamide) and the chiral β-amino-alcohol (see Table 6). For example, a P-R-HBA-*l*-PDMS$_{1.1}$ conetwork takes up 43% more (−)-cinchonidine than the respective P-S-HBA-*l*-PDMS$_{1.1}$ conetwork. The difference of the interaction with the diastereomeric (+)-cinchonine is less pronounced. That can be explained by cooperative hydrogen bonds of the alkaloid.

The release of the alkaloid (−)-cinchonidine was determined by immersing the respective loaded conetwork in chloroform in a stirred UV–vis cuvette and measuring the increase in absorbance at 317 nm. The release rate (also see Table 7) of the alkaloid from

Table 6
Concentration of cinchona alkaloid in the conetworks.

	P-R-HBA-*l*-PDMS1.1	P-S-HBA-*l*-PDMS1.1
	Concentration alkaloid	[μmol/gAPCN]
(−)-cinchonidine	28.4 ± 1.4	19.8 ± 1.1
(+)-cinchonine	25.8 ± 1.3	29.8 ± 1.1

Table 7
Release rate of chinchona alkaloid depending on the conformation of the APCN.

	Initial rate [%release/sec]		Relation (inital rate a/ initial rate b)
	P-R-HBA-*l*-PDMS1.1	P-S-HBA-*l*-PDMS1.1	
(−)-cinchonidine	0.26 ± 0.01	0.84 ± 0.05	4.0 ± 0.5
(+)-cinchonine	1.12 ± 0.06	0.28 ± 0.03	3.2 ± 0.2

P-R-HBA-*l*-PDMS$_{1.1}$ was 0.073 ± 0.002 μmol/s g_{APCN}. This rate is respective to 0.26 ± 0.01%/s of the overall uptake of (−)-cinchonidine. The measured release of the alkaloid from the P-S-HBA-*l*-PDMS$_{1.1}$ was 0.166 ± 0.004 μmol/s g_{APCN}, being 0.84 ± 0.05%/s of the overall uptake. The relation of the release rates corresponds to the relation of the diffusion constants of the molecule. (−)-cinchonidine diffuses 3.2 ± 0.2 times faster off the P-S-HBA-*l*-PDMS$_{1.1}$ APCN compared to the P-R-HBA-*l*-PDMS$_{1.1}$ conetwork. The second used chiral model compound was the alkaloid (+)-cinchonine. The achieved concentration in the networks were 25.8 ± 1.3 μmol/g_{APCN} for P-R-HBA-*l*-PDMS$_{1.1}$ and 29.8 ± 1.1 μmol/g_{APCN} for P-S-HBA-*l*-PDMS$_{1.1}$ network. The release of (+)-cinchonine to chloroform in the case of the P-R-HBA-*l*-PDMS$_{1.1}$ conetwork was determined to be 0.290 ± 0.008 μmol/(s g_{APCN}) (1.12 ± 0.06%/s). In the case of a P-S-HBA-*l*-PDMS$_{1.1}$ conetwork a slower release rate of 0.085 ± 0.009 μmol/s *g* network was observed. This is 0.28 ± 0.03/s of the overall uptake of (+)-cinchonine. The relation of the initial release rates of the release of (+)-cinchonine was as high as 4.0 ± 0.5. These results show clearly that both used alkaloids get in close contact to the hydrophilic phase. Further, the interaction of both enantiomers is obviously attributed to the chirality of the conetworks. While the +CC diffuses four times faster than −CC in the S-APCN, +CC diffuses 3.2 times slower than −CC in an R-APCN.

4. Conclusions

The novel water-soluble polymers poly-(R,S)-*N*-(1-hydroxybutan-2-yl)acrylamide and poly-(R)-*N*-(1-hydroxybutan-2-yl)-acrylamide are LCST polymers in water and precipitate at some 25 °C and above. This makes them very intriguing candidates as chiral and/or thermosensitive phase in an amphiphilic polymer conetwork (APCN). The synthesis of the conetwork by copolymerizing the TMS-protected chiral acrylamide and PDMS crosslinkers of different lengths resulted in clear, transparent, and insoluble elastic materials, indicating a high yield conversion without macroscopic phase separation. All conetworks showed two different T_g values, which is a literature relevant hint for the existence of a phase separation. However, the conetworks with a PDMS crosslinker of some 1100 g/mol did not show distinguishable nanophases in the AFM and exhibited the swelling characteristics of a random polymer network. On the other hand, the conetworks with the PDMS crosslinker of 5620 g/mol formed well-defined nanophases and show the typical morphology-dependent swelling behaviour of an APCN. Thus, two different T_g values are obviously not sufficient to predict nanophase separated materials.

The synthesized P-HBA-*l*-PDMS$_{5.6}$ APCNs show no sharp LCST but a continuous increase of their swellability in water with decreasing temperature in a range of 40–2 °C. Even the swelling in organic solvents can be controlled by temperature. This makes the P-HBA-*l*-PDMS membranes interesting candidates for smart materials and temperature selective separation membranes with tunable MW cut-offs. Detailed investigations regarding these features are part of current research. The chiral conetworks show great potential as separation membranes for racemates. It could be shown on the example of (−)-cinchonidine and (+)-cinchonine that desorption of the molecules from the membranes is strongly dependent on the chirality of the hydrophilic phase, even in an organic solvent.

In closing, the synthesized polymer conetworks P-HBA-*l*-PDMS$_{5.6}$ are perfect APCNs with temperature tunable swelling characteristics and chiral separation potential universal for nearly all solvents.

Acknowledgements

This work was supported by the Deutsche Forschungsgemeinschaft (SFB 428 and the Emmy-Noether-Programm). The authors thank Stephan Dech and Matthias Thiel for their experimental help.

References

[1] Erdodi G, Kennedy JP. Progress in Polymer Science 2006;31(1):1–18.
[2] Domjan A, Erdoedi G, Wilhelm M, Neidhoefer M, Landfester K, Ivan B, et al. Macromolecules 2003;36(24):9107–14.
[3] Bruns N, Scherble J, Hartmann L, Thomann R, Ivan B, Mulhaupt R, et al. Macromolecules 2005;38(6):2431–8.
[4] Ivan B, Almdal K, Mortensen K, Johannsen I, Kops J. Macromolecules 2001; 34(6):1579–85.
[5] Kali G, Georgiou Theoni K, Ivan B, Patrickios Costas S, Loizou E, Thomann Y, et al. Langmuir 2007;23(21):10746–55.
[6] Kafouris D, Gradzielski M, Patrickios CS (Washington, DC, U.S.). Macromolecules 2009;42(8):2972–80.
[7] Ivan B, Kennedy JP, Mackey PW. Acs Symposium Series 1991;469:194–202.
[8] Ivan B, Kennedy JP, Mackey PW. Acs Symposium Series 1991;469:203–12.
[9] Nicolson PC, Vogt J. Biomaterials 2001;22(24):3273–83.
[10] Sun Y, Collett J, Fullwood NJ, Mac Neil S, Rimmer S. Biomaterials 2007;28(4):661–70.
[11] Tanahashi K, Jo S, Mikos AG. Biomacromolecules 2002;3(5):1030–7.
[12] Reyntjens W, Jonckheere L, Goethals E, Du Prez F. Macromolecular Symposia 2001;164(Reactive Polymers):293–300.
[13] Scherble J, Thomann R, Ivan B, Mulhaupt R. Journal of Polymer Science, Part B: Polymer Physics 2001;39(12):1429–36.
[14] Reyntjens WG, Du Prez FE, Goethals EJ. Macromolecular Rapid Communications 1999;20(5):251–5.
[15] Kennedy JP, Fenyvesi G, Na S, Keszler B, Rosenthal KS. ACS Symposium Series 2003;833(Polymer Gels):290–9.
[16] Tiller JC, Sprich C, Hartmann L. Journal of Controlled Release 2005;103(2):355–67.
[17] Hensle EM, Tobis J, Tiller JC, Bannwarth W. Journal of Fluorine Chemistry 2008;129(10):968–73.
[18] Bruns N, Tiller JC. Nano Letters 2005;5(1):45–8.
[19] Savin G, Bruns N, Thomann Y, Tiller JC. Macromolecules 2005;38(18):7536–9.
[20] Bruns N, Bannwarth W, Tiller JC. Biotechnology and Bioengineering 2008;101(1):19–26.
[21] Hanko M, Bruns N, Tiller Joerg C, Heinze J. Analytical and Bioanalytical Chemistry 2006;386(5):1273–83.
[22] Hanko M, Bruns N, Rentmeister S, Tiller Jorg C, Heinze J. Analytical Chemistry 2006;78(18):6376–83.
[23] Keszler B, Kennedy JP, Ziats NP, Brunstedt MR, Stack S, Yun JK, et al. Polymer Bulletin 1992;29(6):681–8.
[24] Erdodi G, Kennedy JP. Journal of Polymer Science, Part A: Polymer Chemistry 2005;43(20):4965–71.
[25] Chen Y, Kennedy JP. Journal of Polymer Science, Part A: Polymer Chemistry 2007;46(1):174–85.
[26] Christova D, Velichkova R, Loos W, Goethals EJ, DuPrez F. Polymer 2003;44(8): 2255–61.
[27] Lequieu W, Du Prez FE. Polymer 2004;45(3):749–57.
[28] Lequieu W, Van de Velde P, Du Prez FE, Adriaensens P, Storme L, Gelan J. Polymer 2004;45(23):7943–51.
[29] Bruns N, Tiller JC. Macromolecules 2006;39(13):4386–94.
[30] Gan D, Mueller A, Wooley KL. Journal of Polymer Science, Part A: Polymer Chemistry 2003;41(22):3531–40.
[31] Gudipati CS, Greenlief CM, Johnson JA, Prayongpan P, Wooley KL. Journal of Polymer Science, Part A: Polymer Chemistry 2004;42(24):6193–208.
[32] Powell KT, Cheng C, Wooley KL, Singh A, Urban MW. Journal of Polymer Science, Part A: Polymer Chemistry 2006;44(16):4782–94.
[33] Xu J, Bohnsack DA, Mackay ME, Wooley KL. Journal of the American Chemical Society 2007;129(3):506–7.
[34] Georgiou TK, Patrickios CS, Groh PW, Ivan B. Macromolecules 2007;40(7): 2335–43.
[35] Girard H, Monjol P. Comptes Rendus Hebdomadaires Des Seances De L Academie Des Sciences Serie C 1974;279(13):553–5.
[36] Porter NA, Allen TR, Breyer RA. Journal of the American Chemical Society 1992;114(20):7676–83.
[37] Aoki T, Muramatsu M, Torii T, Sanui K, Ogata N. Macromolecules 2001;34(10): 3118–9.

[38] Hesse M, Meier H, Zeeh B. Spektroskopische methoden in der organischen chemie. 7th. ed. Stut Tgart: Thieme; 2005.
[39] Mori H, Iwaya H, Nagai A, Endo T. Chemical Communications 2005;38:4872–4.
[40] Liu F, Urban MW. Macromolecules 2008;41(2):352–60.
[41] Hirano T, Okumura Y, Kitajima H, Seno M, Sato T. Journal of Polymer Science, Part A: Polymer Chemistry 2006;44(15):4450–60.
[42] Triftaridou AI, Vamvakaki M, Patrickios CS. Biomacromolecules 2007;8(5): 1615–23.
[43] Brandrup J, Immergut EH. Polymer handbook. New York: Wiley; 1975.
[44] Flory PJ. Principles of polymer chemistry. 1st. ed. New York: Cornell University Press; 1953.
[45] Park D, Keszler B, Galiatsatos V, Kennedy JP. Journal of Applied Polymer Science 1997;66(5):901–10.
[46] Harmon ME, Kuckling D, Pareek P, Frank CW. Langmuir 2003;19(26): 10947–56.
[47] Fu Q, Rao GVR, Ward TL, Lu Y, Lopez GP. Langmuir 2007;23(1):170–4.